



## The Adsorption of Basic Dye (Astrazon Blue FGRL) from Aqueous Solutions Onto Two Different Clays: Talc and Chrysotile

*Bazik Boyanın (Astrazon Mavisi FGRL) İki Farklı Doğal Kil Üzerine Adsorpsiyonu: Talc ve Chrystoline*

Erhan Gengeç\* 

University of Kocaeli Department of Environmental Protection 41275, Kartepe Kocaeli, Turkey

### Abstract

In this study, Talc and Chrysotile were obtained from Sivas, Turkey and used as adsorbents for the investigation of the adsorption of the basic dye (Astrazon Blue FGRL) from aqueous solutions at various dye concentrations (100–400 mg/L), initial pH (3–7), adsorbent doses (1–4 g/L), contact time (2.5–1400 min) and temperatures (313–333 K). The result showed that the adsorption capacity of the dye increased with increasing initial dye concentration, pH, adsorbent dose and temperature. In addition, three kinetic models; the pseudo first order, pseudo second order and intraparticle diffusion, were used to predict the adsorption rate constants. The results showed that the highest correlation coefficients ( $R^2 > 0.9960$ ) were obtained for pseudo second order kinetics. When the natural clays were compared, it was observed that, Talc showed higher removal efficiencies and adsorption capacity than Chrysotile. The highest adsorption capacity was obtained as 284 mg/g and 169 mg/g for Talc and Chrysotile at pH 7, 298 °K, 300 mg/L of initial dye concentration and 1020 min of agitation time, respectively. The results showed that Talc and Chrysotile have important potentials for removal of basic dyes which are cheap and easy available.

**Keywords:** Adsorption kinetics, Basic dyes, Natural clays, Pseudo second order kinetics

### Öz

Bu çalışmada Sivas İlinden temin edilen, Talc ve Chrysotile doğal killerin bazik tekstil boyası (Astrazon Mavisi) giderimdeki kullanım potansiyeli araştırılmıştır. Çalışma kapsamında farklı boya başlangıç konsantrasyonları (100–400 mg/L), pH (3–7), adsorbent miktarı (1–4 g/L) ve sıcaklıklarda (313–333 K) çalışılmıştır. Sonuçlar; artan başlangıç konsantrasyonu, pH, adsorbent miktarı ve sıcaklığın adsorpsiyon kapasitesini artırdığını göstermiştir. İlave olarak, üç kinetik model; yalnızca birinci, yalnızca ikinci ve partikül içi difüzyon modeli adsorpsiyon sabitlerinin hesaplanması için kullanılmıştır. Sonuçlar en yüksek korelasyon katsayılarının ( $R^2 > 0.9960$ ), yalnızca ikinci dereceden kinetik ile elde edildiğini göstermektedir. Doğal killer kıyaslandığında Talc'ın Chrysotile'den daha yüksek giderim verimi ve adsorpsiyon kapasitesine sahip olduğu görülmüştür. pH 7'de, 300 mg/L başlangıç boya konsantrasyonunda ve 1020 dakikalık karıştırma süresinde Talc ve Chrysotile için en yüksek adsorpsiyon kapasiteleri 284 mg/g ve 169 mg/g olarak elde edilmiştir.

**Anahtar Kelimeler:** Adsorpsiyon kinetiği, Bazik boyalar, Doğal kil, Yalnızca ikinci dereceden adsorpsiyon kinetiği

### 1. Introduction

Nowadays, about 10.000 dyes and pigments have been used in textile dyeing processes. From among these, cationic dyes, commonly known as basic dyes are widely used in several types of textile such as acrylic, nylon, silk, and wool. In these processes, a high amount of effluents is produced which contain about 10–15% of the dye. The direct discharge of textile wastewater into the water resources pollutes the water

and affects the aquatic life. The dye contaminated wastewater damage the aesthetic nature of water, decreases the light penetration, and the photosynthetic activity of aquatic organisms. Basic dyes can also cause allergic dermatitis, skin irritation, cancer, and mutations (Marungrueng and Pavasant 2006, Sun and Yang 2003, Karagozoglu et al. 2007, Kobya et al. 2015).

Up till now, the biodegradation, adsorption, precipitation, membrane filtration, chemical degradation, photo-degradation and chemical coagulation processes were used for the treatment of textile wastewater in the literature. However,

\*Corresponding Author: [erhan.gengec@kocaeli.edu.tr](mailto:erhan.gengec@kocaeli.edu.tr)

these techniques have a lot of disadvantages besides advantages. For instance, hydraulic retention time of biological treatments is high, and they are often ineffective for removing due to high toxicity of dyes (Belkacem et al. 2008, Greaves et al. 1999). Membrane filtration provides treatment of dyes with high molecular mass, but dyes with low molecular mass can pass through the membranes, resulting in a considerable cost (Vandevivere et al. 1998, Zahrim et al. 2011). Chemical coagulation leads to the production of large amounts of sludge and undesired reactions during the process (Verma et al. 2012). Chemical degradation by oxidative agents such as chlorine produces very toxic products such as organochlorine compounds (Vandevivere et al. 1998, Bhaskar Raju et al. 2009, Alaton et al. 2002, Szpyrkowicz et al. 2001). Advanced oxidation processes such as photocatalysis, ozonation, UV, Fenton reactive, and ultrasonic oxidation are not preferred because of the high process cost. These techniques usually require additional chemicals, producing a huge volume of sludge and/or secondary pollution. Hence, there is interest in developing cost-effective and eco-friendly alternatives for treatment of effluent from dyeing operations. Adsorption is considered to be most effective and proven technology for the wastewater treatment (Raffiea Baseri et al. 2012). Various adsorbents have been used to remove different types of pollutants from wastewaters, especially which are not easily biodegradable. However, difficulty of separation from the wastewater after use, the regeneration problems, and high cost of adsorbent are major concerns associated with adsorbent. For instance, the activated carbon process is expensive on account of limitations in the regeneration process and the high cost of waste disposal (Vandevivere et al. 1998, Malamis et al. 2011). Thus, there has been growing interest in finding inexpensive and effective alternative to replace the costly adsorbents. Attention has focused on natural clay with low cost. Clay minerals are described as layer-type aluminosilicates that are formed as products of chemical weathering of other silicate minerals at the earth's surface. Clays and clay minerals have been in use as raw materials such as agricultural applications, in engineering and construction applications, in environmental remediation, in geology, pharmaceuticals, food processing, and many other industrial applications (Ismadji et al. 2015). Due to the high surface area and exchange capacities, natural clays such as Talc and Chrysotile have been used frequently in wastewater treatment.

Talc which has  $Mg_3Si_4O_{10}(OH)_2$  chemical formula and foliated, granular, or fibrous shapes, is a layered magnesium silicate mineral. The talc elementary sheet is composed

of octahedral magnesium hydroxide structures. The components in sheets are linked by ionic and covalent bonds (Sprynskyy et al. 2011). Until now, Talc have been used widely in treatment of pollutants such as carboxymethyl cellulose (Khraisheh et al. 2005), uranium (Sprynskyy et al. 2011), polysaccharide (Jenkins and Ralston 1998), lead and cadmium (Huang and Fuerstenau 2001). On the other hand, Chrysotile,  $Mg_3Si_2O_5(OH)_4$ , is composed of sheets of tetrahedral silica in a pseudo-hexagonal network joined to sheets of octahedral co-ordinated magnesium (Yu et al. 2015). Due to their advantages, Chrysotile have been intensively studied in the field of wastewater treatment such as adsorption of sodium dodecylsulfate (Valentim and Joekes 2006), Cu(II) (Liu et al. 2013), Pb(II), Cd (II) and Cr(III) (Yu et al. 2015).

In this study, the removal of Astrozon Blue FGRL (basic dye) was studied with two natural clays (Talc and Chrysotile) which obtained from Sivas City, Turkey. The effect of the variables such as initial pH (pHi), initial dye concentration ( $C_0$ ), sorbent dosage (ms), temperature and contact time (tc) on the adsorption were examined by using a batch method. Several kinetic mechanisms; pseudo first order, pseudo second order and intraparticle diffusion models were applied on data. In addition, SEM, XRD and FTIR were used to characterize the raw and used clays.

## 2. Material and methods

### 2.1. Adsorbents and Dye

Depending on the academic source, there are four main groups of clays: kaolinite, montmorillonite–smectite, illite and chlorite. Talc and Chrysotile are classified in group of smectite and kaolinite, respectively (Bello et al. 2013). In this study, natural Talc and Chrysotile were obtained from Sivas, Turkey and used as adsorbents.

Astrazon Blue FGRL was obtained from Dystar and used for the batch adsorption runs. This dye is a mixture of C.I. Basic Blue 159 and C.I. Basic Blue 3 and the ratio of the two dyes is 5:1 (w/w), respectively. The structures of these two dyes are displayed in Figure 1. AB-FGRL is mainly used as acrylic dyeing in the industry (Karagozoglu et al. 2007).

### 2.2. The Experimental Set-up and Procedure

50 ml of synthetic solutions with different dye concentrations were prepared from stock solution of 1000 mg/L. Then, the pH of the sample was adjusted with 1.0 M  $H_2SO_4$  or 1.0 M NaOH and measured by a pH meter (WTW Inolab pH

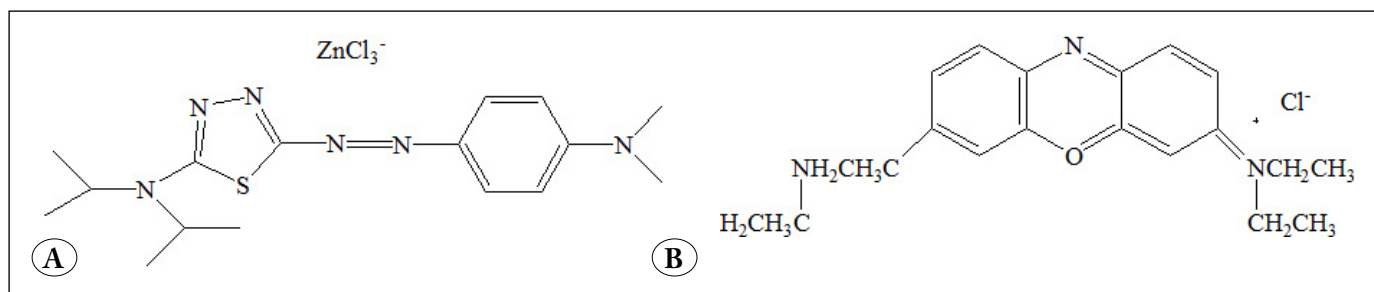


**Figure 1.** Chemical structures of (A) C.I. Basic Blue 159 and (B) C.I. Basic Blue 3 (Karagozogu et al. 2007).

720). Batch adsorption tests were carried out in a NUVE ST-402 model shaker at 240 rpm in order to investigate the adsorption of basic dye onto clays. Samples were filtered at the end of the contact time and remaining dye concentration was analyzed by UV-Vis spectrophotometer at 495 nm (Perkin-Elmer 550 SE). Adsorption efficiency ( $E$ , %) has been calculated according to the following formula:

$$E = \left[ \frac{C_0 - C_e}{C_0} \right] \times 100 \quad (1)$$

where  $C_0$  and  $C_e$  are initial and remaining dye concentrations (mg/L), respectively.

JEOL 6.060 type scanning electron microscopy (SEM) was used to obtain SEM images. Crystal phases of the precipitates were characterized using a XRD diffractometer (Rigaku 2000 D/max with  $Cu_{K\alpha}$ -radiation,  $\lambda = 0.154$  nm at 40 kV and 40mA). Fourier transform infrared (FTIR) spectrum of the clays was recorded in the range 4000-650  $cm^{-1}$  on a Bio Rad FTS 175 C spectrophotometer.

### 2.3. Adsorption Kinetics

The adsorption capacity of adsorbents (mg/g) was calculated using the following relationship:

$$\text{The adsorption capacity of adsorbents, } q_e = \frac{(C_0 - C_e)V}{m} \quad (2)$$

where  $m$  is the mass of clay (g),  $V$  (l) is the volume of wastewater. The study of adsorption kinetics describes the solute uptake rate and evidently this rate controls the residence time of adsorbate uptake at the solid-solution interface. The adsorption rate constants for the dye removal were calculated by using pseudo-first order, second-order and intraparticle diffusion kinetic models (Karagozogu et al. 2007) which were used to describe the mechanism of the adsorption. The relationships between the experimental data and the model-predicted values were expressed by the correlation coefficients ( $R^2$ ). A relatively high  $R^2$  value indicates that the model successfully describes the kinetics of the adsorption.

#### 2.3.1. The Pseudo-First-Order Equation

A pseudo-first-order equation can be expressed in a linear form as;

$$\log(q_e - q_t) = \log(q_e) - \frac{k_1}{2.303} t \quad (3)$$

where  $q_e$  and  $q_t$  are the amount of dye (mg/g) on the adsorbents at the equilibrium and at time  $t$ , respectively, and  $k_1$  is the rate constant of adsorption ( $min^{-1}$ ). Values of  $k_1$  were calculated from the plots of  $\log(q_e - q_t)$  versus  $t$ .

#### 2.3.2. The Pseudo-Second-Order Equation

The pseudo-second-order adsorption kinetic rate equation is expressed as;

$$\frac{dq_t}{dt} = k_2(q_e - q_t)^2 \quad (4)$$

where  $k_2$  is the rate constant of pseudo-second-order adsorption (g/mg min). By integrating and applying the initial conditions, we have a linear form as;

$$\left( \frac{t}{q_t} \right) = \frac{1}{k_2 q_e^2} + \frac{1}{q_e} t \quad (5)$$

where  $q_e$  is the amount of dye at equilibrium (mg/g). The second-order rate constants were used to calculate the initial sorption rate,  $h = k_2 q_e^2$ . Values of  $k_2$  and  $q_e$  were calculated using the intercept and the slope of the linear plots of  $t/q_t$  versus  $t$ .

#### 2.3.3 Intraparticle Diffusion

The rate constant for intraparticle diffusion ( $k_{id}$ ) is calculated using following equation:

$$q = k_3 t^{1/2} + C_i \quad (6)$$

where  $q$  is the amount of dye (mg/g) at time ( $t$ ),  $k_{id}$  (mg/g  $min^{1/2}$ ) is the rate constant for intraparticle diffusion and  $C_i$  is the thickness of the boundary layer. The values of  $k_3$  were calculated from the slope of the linear plots of  $q$  versus  $t^{1/2}$  (Kannan and Sundaram 2001, Rafiq et al. 2014).

## 2.4. Adsorption Isotherms

The adsorption capacities of clays were analyzed with Langmuir and Freundlich isotherms which are well-known adsorption models. The Langmuir and Freundlich isotherm are expressed as the following Eqns (7 and 8), respectively.

$$\frac{C_e}{q_e} = \frac{1}{kV_m} + \frac{C_e}{V_m} \quad (7)$$

$$\log q_e = \log K_f + \frac{\log C_e}{n} \quad (8)$$

where  $q_e$  represents the mass of adsorbed dye per unit clay (mg/g),  $V_m$  is the monolayer capacity,  $k$  is the equilibrium constant and  $C_e$  is the equilibrium concentration of the solution (mg/L).  $k$  and  $V_m$  is determined from the plot of  $\frac{C_e}{q_e}$  against  $C_e$ .  $K_f$  (mmol/g) and  $\frac{1}{n}$  are Freundlich isotherm constants and the plot of  $\log q_e$  against  $\log C_e$  shows data for adsorption of dye onto clay is fitting well to the Freundlich isotherm (Alyüz and Veli 2009).

## 3. Results and Discussion

### 3.1. Adsorption Isotherm

In this study, the effect of initial pH, initial dye concentration, sorbent dosage, contact time and temperature on adsorption rate and removal efficiencies were evaluated. In adsorption study, adsorption isotherm equations; Langmuir and Freundlich were applied. The adsorption isotherm data of AB-FGRL could not be described by isotherm equations of Langmuir and Freundlich. Plots of  $C_e/q_e$  vs.  $C_e$  and  $\log q_e$  vs.  $\log C_e$  were not line. The fitness between experimental data and theoretical models was not good ( $R^2 < 0.93$ ). This result is similar to that of Yang et al (Sun and Yang 2003).

### 3.2. Effect of Initial pH

pH is one of the most important parameters that affect the interaction between the adsorbent and adsorbate. It had been proven that the adsorption system depended on the degree of ionization of the dye solution and the dissociation of functional groups on the active sites of the adsorbent which varied at different pH.

To search for the optimal pH, the adsorptions of AB-FGRL were realized at various pH (3, 5, 7). There were no attempts to examine the adsorption at basic conditions (pH > 7) as the dyes could not be dissolved completely (Pimol et al. 2008). As seen in Figure 2, adsorption capacities were increased with the increased pH values and the effect of pH was significant. The adsorption capacity changed from 58.0 to 103.2 mg/g for Chrysotile and 53.6 to 103.4 mg/g for Talc

with an increase in the pH from 3 to 7. These phenomena can be explained as the adsorption of basic dyes decreased at lower pH due to the occurrence of proton in acidic mediums (Pimol et al. 2008).

On the other hand, the values of rate constants were obtained from three kinetic models.  $R^2$  and  $q$  values for the AB-FGRL were given in Tables 1–2. In tables 1-2, the linear correlation values ( $R^2$ ) close to 1 showed that the model was statistically significant and indicated the applicability of these kinetic equations. The  $R^2$  values for the pseudo-first order and the intraparticle diffusion model were varying at a high range and lower than that of pseudo-second order. All  $R^2$  values for pseudo-second order were obtained as >0.9960. The pseudo-second order model fitted well and suggested chemical sorption as the rate-limiting step of the adsorption mechanism and no involvement of a mass transfer in solution (Gengec 2015).

### 3.3. Effect of Initial AB-FGRL Concentration

It is well known that the dye removal efficiencies and adsorption capacities are dependent on the concentration of the dye (Karagozoglu et al. 2007). Thus, the effects of initial dye concentrations on the rate of adsorption were studied in this study (Figure 3). The increased initial dye concentration from 200 to 400 mg/L caused an increase in the adsorbed dye amount from 99.8 to 197.0 mg/g for Talc and from 98.3 to 162.44 mg/g for Chrysotile. Moreover, the initial rate of adsorption was greater for higher initial dye concentration. This phenomena can be explained as the increased mass driving force is decreased the resistance to the dye uptake (Karagozoglu et al. 2007).

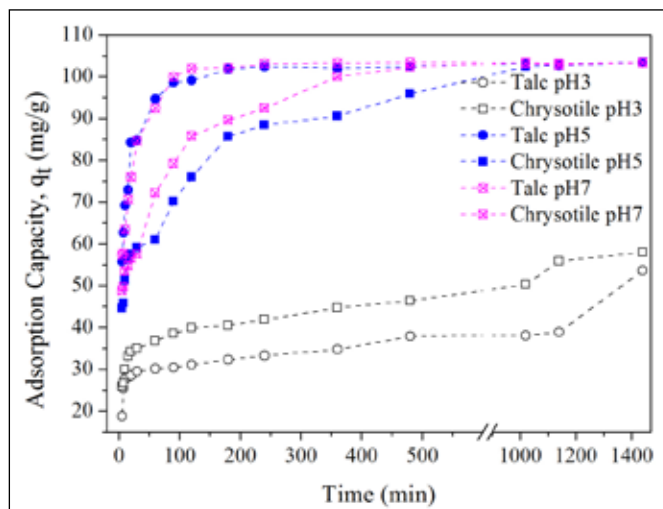


**Figure 2.** Effect of initial pH on AB-FGRL adsorption ( $C_0$ : 200 mg/L,  $m_s$ : 2 g/L, T: 298 °K and : 240 rpm).

**Table 1.** The model parameters of pseudo first order, pseudo second order and intraparticle diffusion for Chrysotile.

Chrysotile															
	Pseudo First Order			Pseudo Second Order			Intraparticle Diffusion								
	$q_{e,cal}$	$k_1$	$R^2$	$q_{e,exp}$	$k_2$	$h$	$R^2$	$q_{e,cal}$	$k_3$	$C_i$	$R^2$	$q_{e,exp}$			
pH	3	37.3	0.002671	0.9670	33.1	50.0	0.0010	2.43	0.9964	50.2	29.5	0.7767	28.996	0.9381	58.0
	5	49.4	0.003915	0.9818	102.4	103.1	0.0004	3.91	0.9968	102.4	63.8	1.6811	50.931	0.8742	103.4
	7	57.1	0.009673	0.9939	85.7	104.2	0.0005	5.69	0.9965	103.2	62.0	1.6342	55.375	0.7879	103.2
$C_0$ (mg/L)	200	68.6	0.004836	0.9807	97.0	52.1	0.0038	10.18	0.9975	50.2	80.0	2.5038	29.222	0.9452	98.3
	300	104.3	0.003455	0.9936	130.8	59.9	0.0027	9.81	0.9975	57.9	122.1	3.8221	26.685	0.9683	138.5
	400	127.4	0.003915	0.9815	156.56	69.9	0.0028	13.77	0.9972	67.2	141.7	4.4361	31.884	0.9739	162.4
	1	120.5	0.000921	0.9466	81.6	66.7	0.0032	14.06	0.9974	65.5	47.7	2.1774	41.355	0.9948	169.6
$m_s$ (g/L)	3	68.3	0.004606	0.9783	87.5	48.5	0.0060	14.16	0.9988	46.9	68.8	3.1392	24.942	0.9792	99.4
	4	48.9	0.008751	0.9945	73.1	76.3	0.0005	3.13	0.9988	74.16	33.7	2.1774	41.355	0.9948	74.2
T (°K)	313	87.9	0.008521	0.9885	97.7	140.9	0.0002	4.60	0.9973	139.4	59.6	6.2797	38.478	0.9954	139.4
	323	75.3	0.008982	0.9754	147.9	151.5	0.0004	9.48	0.9998	149.1	90.9	8.3013	43.279	0.9832	149.1
	333	84.6	0.016582	0.9819	136.6	151.5	0.0006	13.04	0.9970	146.6	83.4	10.763	40.927	0.9837	148.9

**Table 2.** The model parameters of pseudo first order, pseudo second order and intraparticle diffusion for Talc.

Talc															
	Pseudo First Order			Pseudo Second Order			Intraparticle Diffusion								
	$q_{e,cal}$	$k_1$	$R^2$	$q_{e,exp}$	$k_2$	$h$	$R^2$	$q_{e,cal}$	$k_3$	$C_i$	$R^2$	$q_{e,exp}$			
pH	3	46.1	0.059648	0.9468	27.8	38.91	0.0015	2.23	0.9984	38.9	31.1	9.832	-2.698	0.9538	27.8
	5	44.1	0.025794	0.9596	98.6	103.09	0.0020	20.75	0.9999	103.4	53.1	11.867	29.853	0.9695	84.2
	7	52.8	0.029709	0.9936	101.9	103.09	0.0021	22.17	0.9999	103.4	40.2	8.984	35.420	0.9659	75.9
$C_0$ (mg/L)	200	76.6	0.019806	0.9790	91.4	102.04	0.0006	5.83	0.9998	99.8	78.2	10.091	2.855	0.9592	78.8
	300	110.3	0.011515	0.9634	141.3	153.85	0.0002	5.56	0.9998	149.8	124	16.010	-11.594	0.9566	107.9
	400	169.3	0.009903	0.9823	178.91	208.33	0.0001	4.37	0.9995	197.0	170	15.540	-12.868	0.9912	156.3
	1	261.5	0.003915	0.9828	154.3	68.03	0.0016	7.40	0.9975	59.0	257.9	11.773	-7.651	0.9850	254.0
$m_s$ (g/L)	3	81.1	0.036387	0.9993	53.2	100.00	0.0009	8.86	0.9997	98.2	76.8	13.269	2.967	0.9626	72.4
	4	42.4	0.032012	0.9876	72.62	75.19	0.0024	13.55	0.9999	74.2	45.5	8.306	16.727	0.9534	61.0
T (°K)	313	80.4	0.037769	0.9971	139.9	149.25	0.0014	32.26	0.9999	147.9	82.3	10.627	60.308	0.9800	139.9
	323	138.6	0.143477	0.9999	115.2	149.25	0.0025	55.87	0.9999	148.0	97.5	21.790	38.702	0.9161	131.1
	333	107.0	0.16858	0.9781	129.5	149.25	0.0026	56.82	0.9999	148.0	86.0	27.198	42.837	0.9932	129.5

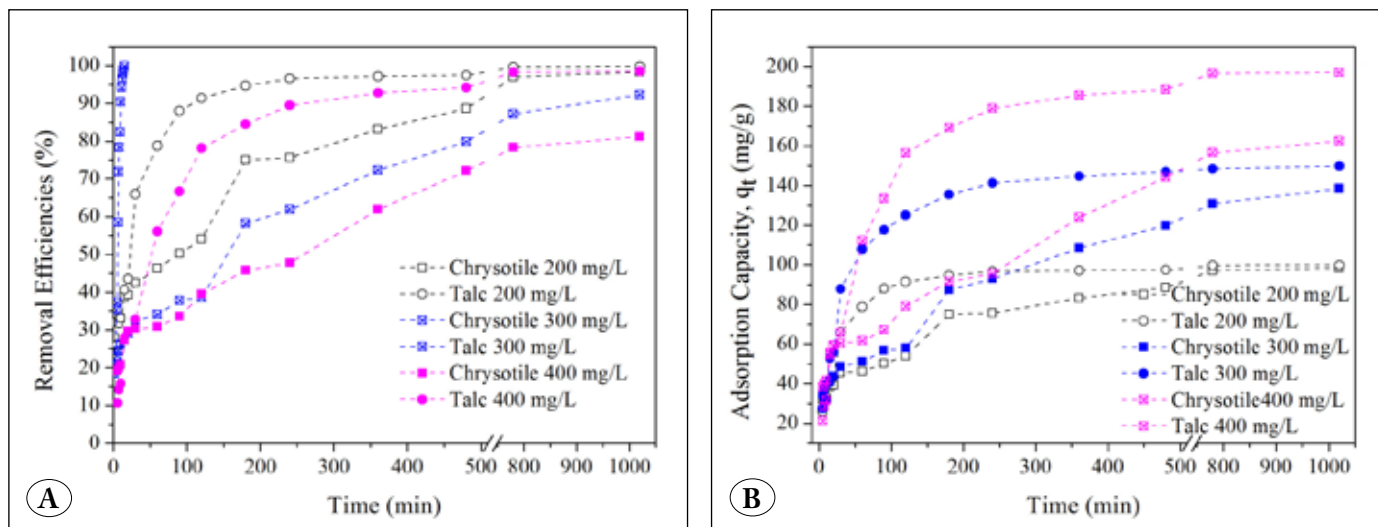


**Figure 3.** Effect of initial dye concentration (pH: 7,  $m_0$ : 2 g/L, T: 303 °K and w: 240 rpm).

Eqs. (2)–(6) were applied to the experimental data for the adsorption of the AB-FGRL onto Talc and Chrysotile. It was clear from the data; the adsorption of the dye onto the adsorbents follows the pseudo second order model. The agreement between the experimental and predicted curves is extremely good. Hence, the concentration of the basic dye in the solution had a strong influence on the pseudo second order kinetics. This model also assumes the rate limiting step may be the adsorption in agreement with chemical adsorption being the rate controlling step, which may involve valence forces through sharing or exchange of electrons between dye and adsorbent (Karagozoglu et al. 2007).

### 3.4. Effect of Adsorbent Dose

The adsorbent dose was varied from 1 to 4 g/L for observing the effect of dose on removal efficiencies and adsorption capacity of clays, when the other factors were held constant. The results showed that an enhancement in adsorption was obtained with the increase in dose of the adsorbent (Figure 4). The results showed that Talc had a higher potential than Chrysotile for removing of basic dyes. The removal efficiencies from 56.53% to 99.71% were obtained by increased amount of Chrysotile from 1 g/L to 4 g/L during 1020 min. On the other hand, the high removal efficiencies (>94 %) were obtained at 1020, 780 and 360 min. for 1 g/L, 3 g/L and 4 g/L of Talc., respectively. The highest adsorbent dose of Talc, the lowest contact time.

Three kinetic models (pseudo - first, -second and intraparticle diffusion) were applied to the results of adsorbent dose (Tables 1–2). The data showed well agreement with the

pseudo second order kinetic model for both of natural clays in terms of higher correlation coefficients ( $R^2 > 0.9960$ ) and the dye adsorption process appeared to be controlled by the chemical process.

### 3.5. Effect of Temperature

The temperature is another driving force in adsorption of basic dye. As seen in Figure 5, while temperature was increased, the removal efficiencies and the adsorption capacity increased. This phenomenon was very clear for Chrysotile. Probably, adsorption increased with further increasing of the temperature due to the increased surface activity. The increased temperature was proved the quick removal of basic dye. The higher removal efficiencies than 92% were obtained at 1020., 180., and 120. min by Chrysotile and 60., 35. and 30. min. by Talc at 313, 323, and 333 °K, respectively.

As mentioned before, Astrazon Blue FGRL (basic dye) is water –soluble cationic dyes. The pseudo–second order model fitted well with experimental results and suggested chemical sorption. The adsorption of Astrazon Blue FGRL on surface of Talc and Chrysotile probably depends on interaction between positive charges of dyes and negative charges of natural clays. Briefly, the adsorption mechanism of basic dyes on Talc and Chrysotile depend on three critical steps:

- Migration of basic dyes on the surface of the clays
- Diffusion of basic dye to the boundary layer of the clays
- Chemical sorption of the dyes by the interaction between

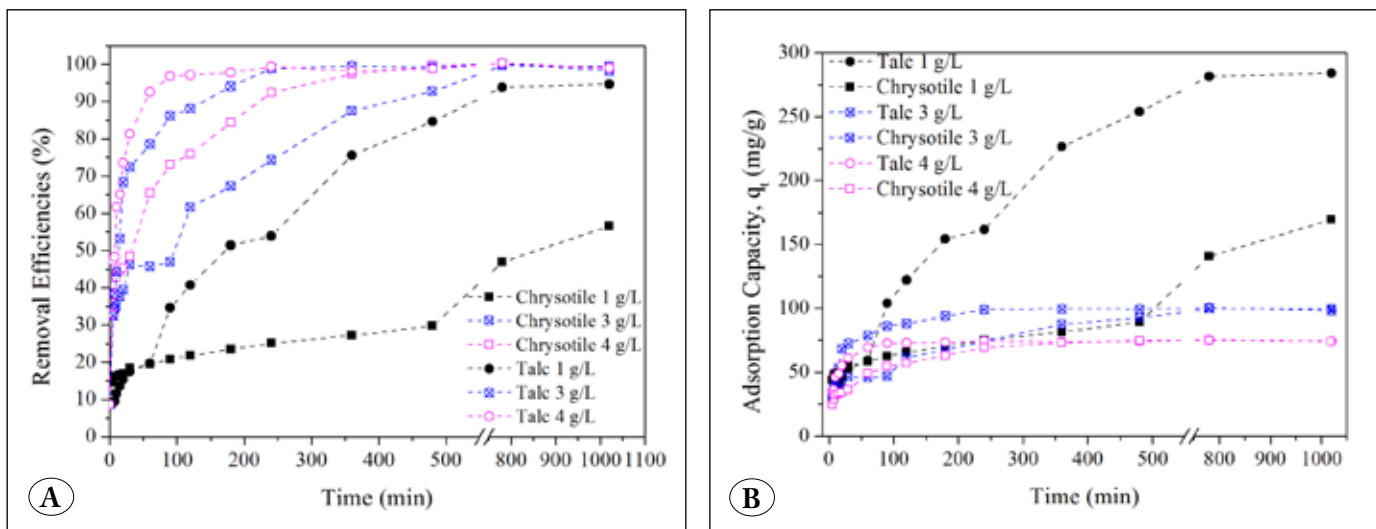


**Figure 4.** Effect of adsorbent dose on (A) removal efficiencies and (B) adsorption capacity ( $C_0$ : 300 mg/L, pH: 7, T: 298 °K and w: 240 rpm).

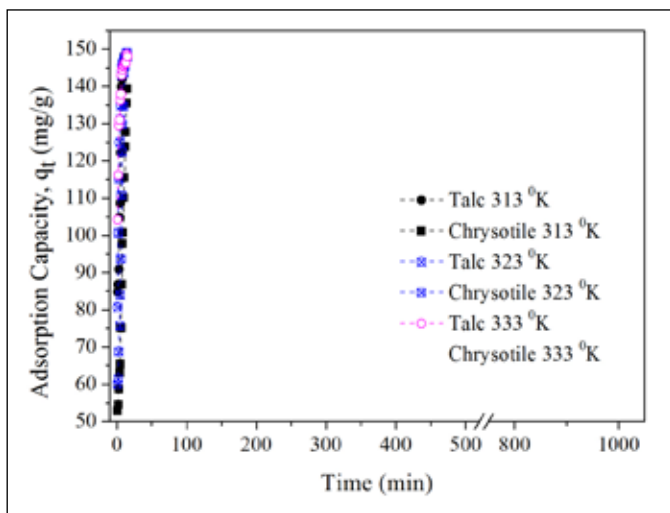


**Figure 5.** Effect of adsorbent dose ( $C_0$ : 300 mg/L,  $m_s$ : 2 g/L, pH: 7, and w: 240 rpm).

polar functional groups on the sorbent surface and dyes (Karagozoglu et al. 2007; Ho and McKay 1998; Doğan et al. 2004)

Consequently, the investigation of the basic dye (Astrazon Blue FGRL) adsorption from aqueous solutions at various dye concentrations, initial pH, adsorbent doses and temperatures by Talc and Chrysotile showed that these two natural clays had favorably capacities for removal of basic dyes. One of the higher adsorption capacities for Astrazon Blue in literature was obtained by Talc (Table 3).

### 3.6. Morphology and Characterization

Talc is a layered magnesium silicate mineral with the chemical formula  $Mg_3Si_4O_{10}(OH)_2$ . The talc elementary sheet is composed of octahedral magnesium hydroxide structures sandwiched between sheets of silicon-oxygen

**Table 3.** Comparison of sorption capacity of Astrazon Blue onto various sorbents.

Adsorbent	$q_{max}$ (mg/g)	Reference
Sepiolite	312.5	(Ongen et al. 2012)
Maize Cob/maize cob	160	(Elgeundi 1991)
Sphagnum Moss Peat	375	(Ho and McKay 1998)
Macroalga <i>C. lentillifera</i>	49.2	(Marungrueng and Pavasant 2006)
Macroalga <i>C. lentillifera</i>	94.34	(Pimol et al. 2008)
Sepiolite, Apricot Shell Activated Carbon, Fly Ash	209, 202 and 152	(Karagozoglu et al. 2007)
Talc and Chrysotile	284 and 169	In this study
Biomass of Baker's Yeast	70	(Farah et al. 2007)
Commercial Activated Carbon	18.5	(Farah et al. 2007)
Mineral waste obtained from coal mining	97.18	(dos Santos et al. 2016)

tetrahedral in which the components are linked by ionic and covalent bonds (Sprynskyy et al. 2011). The mineral structure of talc showed the presence of talc, dolomite and quartz (Figure 6).

On the other hand, Chrysotile is a fibrous hydrated magnesium silicate ( $Mg_3Si_2O_5(OH)_4$ ) consisting of octahedral sheets of brucite ( $Mg(OH)_2$ ) covalently bonded to tetrahedral sheets of tridymite ( $SiO_4$ ) (Valentim and Joekes 2006) and the mineral structure of chrysotile showed the presence of hrysotile, calcite and quartz (Figure 6).

The FTIR spectra demonstrated the characteristic bands at 3675, 1572, 1536, 1425, 1270, 1165, 1012, 880, 800, 775, 725, and 670  $cm^{-1}$  for Talc and 3685, 3654, 1042, and 944  $cm^{-1}$  for Chrysotile (Figure 7A). The bands at 3685  $cm^{-1}$ , 3675

$cm^{-1}$ , and 3433  $cm^{-1}$  correspond to the stretching vibration of hydroxyl in the magnesium hydroxide, vibrations of Mg-OH groups, and vibrations of the Si-OH groups, respectively. The bands at 1080–970  $cm^{-1}$  originate from the Si-O-Si, Si-O-Mg and Si-O stretching frequencies and the stretching vibration of Si-O-Mg linkages became apparent at 670  $cm^{-1}$ . On the other hand, dolomite impurities resulted in 1443  $cm^{-1}$  (Ongen et al. 2012, Sprynskyy et al. 2011, Valentim and Joekes 2006). It was clear that the clays displayed a number of absorption peaks, reflecting the complex nature of the adsorbent.

It was clear from the spectra of raw and used clay (Figure 7b), new peaks such as 1165  $cm^{-1}$  (C-N stretch), 1260  $cm^{-1}$  (Si-C stretch) and 1530  $cm^{-1}$  (NH deformation) were formed.

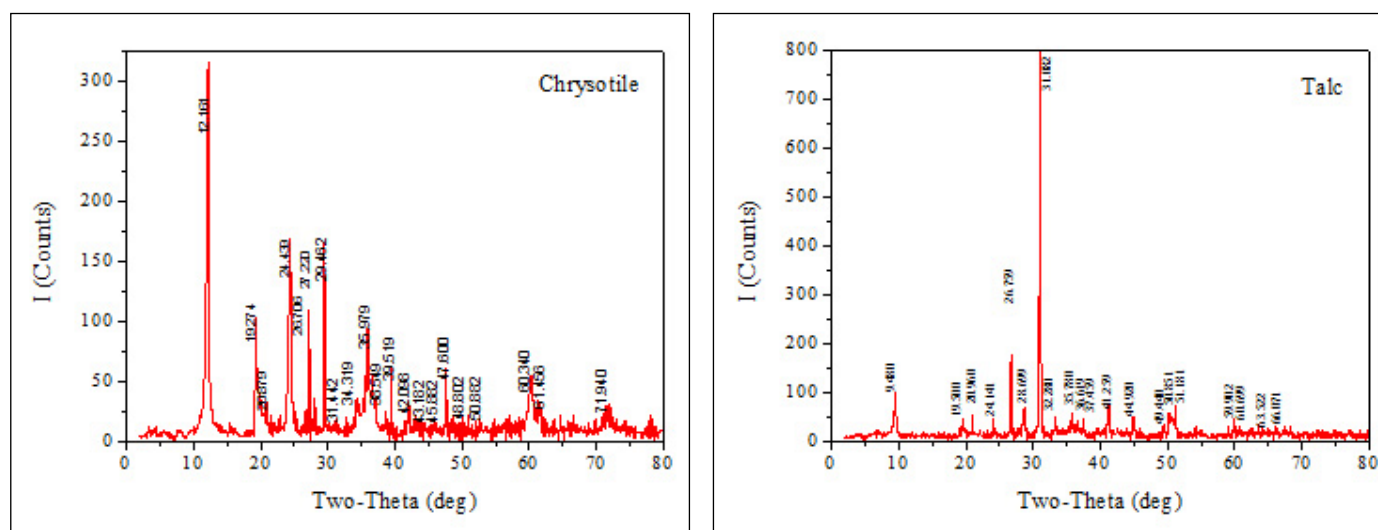


Figure 6. X-ray diffraction spectrum of the natural clays.

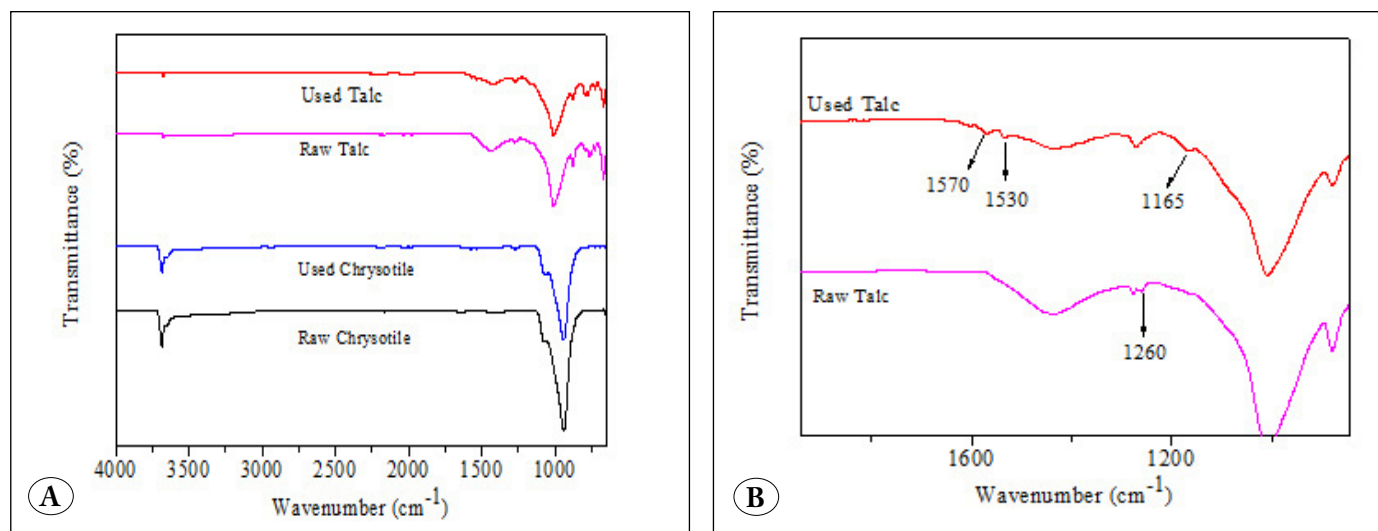


Figure 7. FTIR spectra of Talc and Chrysotile.



These new peaks in the spectrum indicated the possible involvement of those functional groups on the surface of the clays in sorption process (Hameed et al. 2008).

In this study, a scanning electron microscope (SEM) was used to characterize the surface of the Talc and Chrysotile at a very high magnification and an accelerating voltage of 15 kV. Samples were coated with gold using a sputter coater with conductive materials to improve the quality of the micrograph. The morphology of Talc and Chrysotile was illustrated in Figure 8 (A and C) showed the SEM image of raw Chrysotile and Talc with a magnification of 10.000.

For comparison, the SEM image of Chrysotile after the adsorption of basic dye were recorded (Figure 8B, D). The results displayed that the chrysotile had typical nano-fibrous morphology which had a cylindrical shape with a length of about 500 nm and Talc had a foliated structure. It is clear from SEM image that the hollows in Talc and Chrysotile were fulfilled during sorption process.

#### 4. Conclusions

The removals of the basic dye by Talc and Chrysotile were studied and the results showed that adsorption capacities were dependent on the initial dye concentration, pH, contact time, temperature and sorbent dosage. As a briefly, the increase in the initial dye concentration, pH, contact time, temperature and sorbent dosage increased the amount of the basic dye adsorbed on the adsorbents. A comparison of kinetic models on the overall adsorption rate showed that dye/adsorbent system was best described by the pseudo second order rate model. Equations were developed using the pseudo-second-order model that accurately predict the amount of the basic dye adsorbed at any contact time, initial dye concentration, initial dye concentration and adsorbent dose within the given range. The experimental results showed that these two natural clays have an important potential as an adsorbent in the removal of the basic dyes. They are cheap, naturally abundant and locally available adsorbents. .

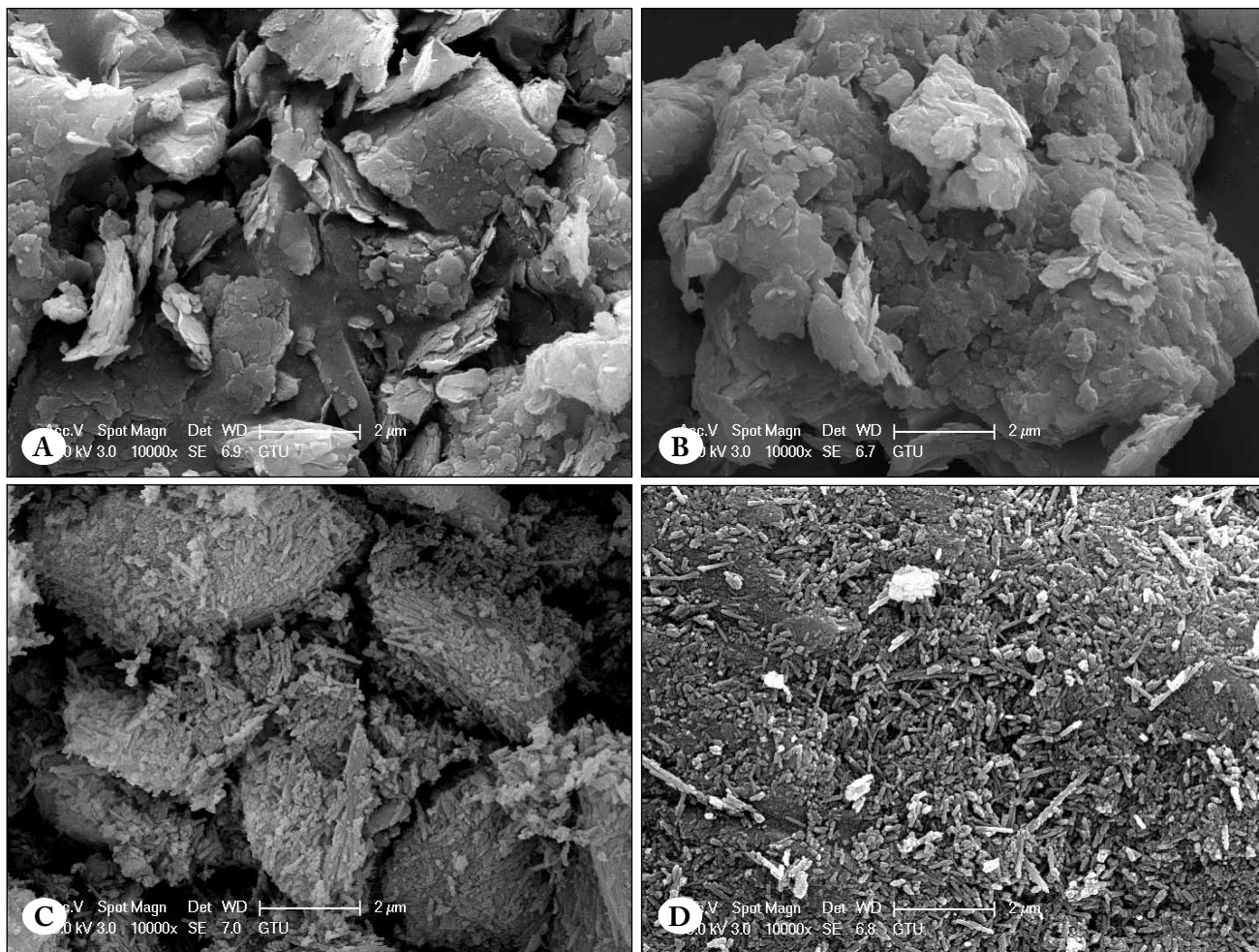


Figure 8. SEM images of raw Talc (A), used Talc (B), raw Chrysotile, and used Chrysotile.

## 5. References

- Alaton, I.A., Balcioglu, I.A. & Bahnemann, D.W., 2002. Advanced oxidation of a reactive dyebath effluent: Comparison of O<sub>3</sub>, H<sub>2</sub>O<sub>2</sub>/UV-C and TiO<sub>2</sub>/UV-A processes. *Water Research*, 36(5), pp.1143–1154.
- Alyüz, B. & Veli, S., 2009. Kinetics and equilibrium studies for the removal of nickel and zinc from aqueous solutions by ion exchange resins. *Journal of Hazardous Materials*, 167(1–3), pp.482–488.
- Belkacem, M., Khodir, M. & Abdelkrim, S., 2008. Treatment characteristics of textile wastewater and removal of heavy metals using the electroflotation technique. *Desalination*, 228(1–3), pp.245–254. Available at: <http://www.sciencedirect.com/science/article/pii/S0011916408002506> [Accessed May 23, 2016].
- Bello, O.S., Bello, I.A. & Adegoke, K.A., 2013. Adsorption of dyes using different types of sand: A review. *South African Journal of Chemistry*, 66(SEPTEMBER), p.0. Available at: [http://www.scielo.org.za/scielo.php?script=sci\\_arttext&pid=S0379-43502013000100024&nrn=iso](http://www.scielo.org.za/scielo.php?script=sci_arttext&pid=S0379-43502013000100024&nrn=iso).
- Bhaskar Raju, G. et al., 2009. Electrochemical pretreatment of textile effluents and effect of electrode materials on the removal of organics. *Desalination*, 249(1), pp.167–174. Available at: <http://dx.doi.org/10.1016/j.desal.2008.08.012>.
- Doğan, M. et al., 2004. Kinetics and mechanism of removal of methylene blue by adsorption onto perlite. *Journal of Hazardous Materials*, 109(1–3), pp.141–148.
- Gengec, E., 2015. Color removal from anaerobic/aerobic treatment effluent of bakery yeast wastewater by polyaniline/beidellite composite materials. *Journal of Environmental Chemical Engineering*, 3(4), pp.2484–2491. Available at: <http://linkinghub.elsevier.com/retrieve/pii/S2213343715002390>.
- Greaves, A.J., Phillips, D.A.S. & Taylor, J.A., 1999. Correlation between the bioelimination of anionic dyes by an activated sewage sludge with molecular structure. Part 1: Literature review. *Journal of the Society of Dyers and Colourists*, 115(12), pp.363–365.
- Hameed, B.H., Mahmoud, D.K. & Ahmad, A.L., 2008. Equilibrium modeling and kinetic studies on the adsorption of basic dye by a low-cost adsorbent: Coconut (*Cocos nucifera*) bunch waste. *Journal of Hazardous Materials*, 158(1), pp.65–72.
- Ho, Y.S. & McKay, G., 1998. The kinetics of sorption of basic dyes from aqueous solution by sphagnum moss peat. *The Canadian journal of chemical engineering*, 76(4), pp.822–827.
- Huang, P. & Fuerstenau, D.W., 2001. The effect of the adsorption of lead and cadmium ions on the interfacial behavior of quartz and talc. *Colloids and Surfaces A: Physicochemical and Engineering Aspects*, 177(2–3), pp.147–156.
- Ismadji, S., Soetaredjo, F.E. & Ayucitra, A., 2015. *Clay Materials for Environmental Remediation*, Available at: [https://books.google.com.tr/books/about/Clay\\_Materials\\_for\\_Environmental\\_Remedia.html?id=b6qgBwAAQBAJ&pgis=1](https://books.google.com.tr/books/about/Clay_Materials_for_Environmental_Remedia.html?id=b6qgBwAAQBAJ&pgis=1) [Accessed January 31, 2017].
- Jenkins, P. & Ralston, J., 1998. The adsorption of a polysaccharide at the talc–aqueous solution interface. *Colloids and Surfaces A: Physicochemical and Engineering Aspects*, 139(1), pp.27–40.
- Kannan, N. & Sundaram, M.M., 2001. Kinetics and mechanism of removal of methylene blue by adsorption on various carbons—a comparative study. *Dyes and Pigments*, 51(1), pp.25–40.
- Karagozoglu, B. et al., 2007. The adsorption of basic dye (Astrazon Blue FGRL) from aqueous solutions onto sepiolite, fly ash and apricot shell activated carbon: Kinetic and equilibrium studies. *Journal of Hazardous Materials*, 147(1–2), pp.297–306.
- Khraisheh, M. et al., 2005. Effect of molecular weight and concentration on the adsorption of CMC onto talc at different ionic strengths. *International Journal of Mineral Processing*, 75(3–4), pp.197–206.
- Kobyas, M., Gengec, E. & Demirbas, E., 2015. Operating parameters and costs assessments of a real dyehouse wastewater effluent treated by a continuous electrocoagulation process. *Chemical Engineering and Processing: Process Intensification*, 101, pp.87–100. Available at: <http://dx.doi.org/10.1016/j.cep.2015.11.012>.
- Liu, K. et al., 2013. Adsorption of Cu(II) ions from aqueous solutions on modified chrysotile: Thermodynamic and kinetic studies. *Applied Clay Science*, 80–81, pp.38–45. Available at: <http://dx.doi.org/10.1016/j.clay.2013.05.014>.
- Malamis, S., Katsou, E. & Haralambous, K.J., 2011. Evaluation of the Efficiency of a Combined Adsorption–Ultrafiltration System for the Removal of Heavy Metals, Color, and Organic Matter from Textile Wastewater. *Separation Science and Technology*, 46(6), pp.920–932. Available at: <http://www.informaworld.com/10.1080/01496395.2010.551166>.
- Marungrueng, K. & Pavasant, P., 2006. Removal of basic dye (Astrazon Blue FGRL) using macroalga *Caulerpa lentillifera*. *Journal of Environmental Management*, 78(3), pp.268–274.
- Ongen, A. et al., 2012. Adsorption of Astrazon Blue FGRL onto sepiolite from aqueous solutions. *Desalination and Water Treatment*, 40(1–3), pp.129–136.
- Pimol, P., Khanidtha, M. & Prasert, P., 2008. Influence of particle size and salinity on adsorption of basic dyes by agricultural waste: dried Seagrass (*Caulerpa lentillifera*). *Journal of Environmental Sciences*, 20(6), pp.760–768.
- Raffiea Baseri, J., Palanisamy, P.N. & Sivakumar, P., 2012. Application of polyaniline nano composite for the adsorption of acid dye from aqueous solutions. *E-Journal of Chemistry*, 9(3), pp.1266–1275.

- Rafiq, Z. et al., 2014. Utilization of magnesium and zinc oxide nano-adsorbents as potential materials for treatment of copper electroplating industry wastewater. *Journal of Environmental Chemical Engineering*, 2(1), pp.642–651.
- Sprynskyy, M. et al., 2011. Adsorption performance of talc for uranium removal from aqueous solution. *Chemical Engineering Journal*, 171(3), pp.1185–1193. Available at: <http://dx.doi.org/10.1016/j.cej.2011.05.022>.
- Sun, Q. & Yang, L., 2003. The adsorption of basic dyes from aqueous solution on modified peat-resin particle. *Water Research*, 37(7), pp.1535–1544.
- Szpyrkowicz, L., Juzzolino, C. & Kaul, S.N., 2001. A comparative study on oxidation of disperse dyes by electrochemical process, ozone, hypochlorite and fenton reagent. *Water Research*, 35(9), pp.2129–2136.
- Valentim, I.B. & Joekes, I., 2006. Adsorption of sodium dodecylsulfate on chrysotile. *Colloids and Surfaces A: Physicochemical and Engineering Aspects*, 290(1–3), pp.106–111.
- Vandevivere, P.C., Bianchi, R. & Verstraete, W., 1998. Review Treatment and Reuse of Wastewater from the Textile Wet-Processing Industry: Review of Emerging Technologies. *J. Chem. Technol. Biotechnol.*, 72, pp.289–302.
- Verma, A.K., Dash, R.R. & Bhunia, P., 2012. A review on chemical coagulation/flocculation technologies for removal of colour from textile wastewaters. *Journal of Environmental Management*, 93(1), pp.154–168. Available at: <http://dx.doi.org/10.1016/j.jenvman.2011.09.012>.
- Yu, S. et al., 2015. Synthesis of magnetic chrysotile nanotubes for adsorption of Pb(II), Cd(II) and Cr(III) ions from aqueous solution. *Journal of Environmental Chemical Engineering*, 3(2), pp.752–762. Available at: <http://dx.doi.org/10.1016/j.jece.2015.03.023>.
- Zahrim, A.Y., Tizaoui, C. & Hilal, N., 2011. Coagulation with polymers for nanofiltration pre-treatment of highly concentrated dyes: A review. *Desalination*, 266(1–3), pp.1–16. Available at: <http://dx.doi.org/10.1016/j.desal.2010.08.012>.